

Aerosols Transmit Prions to Immunocompetent and Immunodeficient Mice

Johannes Haybaeck^{1,9a}, Mathias Heikenwalder^{1,9b}, Britta Klevenz^{2,9}, Petra Schwarz¹, Ilan Margalith¹, Claire Bridel¹, Kirsten Mertz^{1,3}, Elizabeta Zirdum², Benjamin Petsch², Thomas J. Fuchs⁴, Lothar Stitz^{2,*}, Adriano Aguzzi^{1,*}

1 Department of Pathology, Institute of Neuropathology, University Hospital Zurich, Zurich, Switzerland, **2** Institute of Immunology, Friedrich-Loeffler-Institut, Tübingen, Germany, **3** Department of Pathology, Clinical Pathology, University Hospital Zurich, Zurich, Switzerland, **4** Department of Computer Science, Machine Learning Laboratory, ETH Zurich, Zurich, Switzerland

Abstract

Prions, the agents causing transmissible spongiform encephalopathies, colonize the brain of hosts after oral, parenteral, intralingual, or even transdermal uptake. However, prions are not generally considered to be airborne. Here we report that inbred and crossbred wild-type mice, as well as *tga20* transgenic mice overexpressing PrP^C, efficiently develop scrapie upon exposure to aerosolized prions. NSE-PrP transgenic mice, which express PrP^C selectively in neurons, were also susceptible to airborne prions. Aerogenic infection occurred also in mice lacking B- and T-lymphocytes, NK-cells, follicular dendritic cells or complement components. Brains of diseased mice contained PrP^{Sc} and transmitted scrapie when inoculated into further mice. We conclude that aerogenic exposure to prions is very efficacious and can lead to direct invasion of neural pathways without an obligatory replicative phase in lymphoid organs. This previously unappreciated risk for airborne prion transmission may warrant re-thinking on prion biosafety guidelines in research and diagnostic laboratories.

Citation: Haybaeck J, Heikenwalder M, Klevenz B, Schwarz P, Margalith I, et al. (2011) Aerosols Transmit Prions to Immunocompetent and Immunodeficient Mice. *PLoS Pathog* 7(1): e1001257. doi:10.1371/journal.ppat.1001257

Editor: David Westaway, University of Alberta, Canada

Received: March 22, 2010; **Accepted:** December 13, 2010; **Published:** January 13, 2011

Copyright: © 2011 Haybaeck et al. This is an open-access article distributed under the terms of the Creative Commons Attribution License, which permits unrestricted use, distribution, and reproduction in any medium, provided the original author and source are credited.

Funding: This work was supported in part by EU grants ANTEPRION and PRIORITY (LS), and the TSE-Forschungsprogramm des Landes Baden-Wuerttemberg, Germany (LS). This work was also supported by grants from the UK Department of Environment, Food and Rural Affairs (AA), the EU grants LUPAS and PRIORITY (AA), the Novartis Research Foundation (AA), and an Advanced Grant of the European Research Council to AA. MH was supported by the Foundation for Research at the Medical Faculty, the Prof. Dr. Max-Cloetta foundation and the Bonizzi-Theler Foundation. The funders had no role in study design, data collection and analysis, decision to publish, or preparation of the manuscript.

Competing Interests: The authors have declared that no competing interests exist.

* E-mail: adriano.aguzzi@usz.ch (AA); lothar.stitz@fli.bund.de (LS)

^{9a} Current address: Institute of Pathology, Medical University Graz, Graz, Austria

^{9b} Current address: Institute of Virology, Technical University München/Helmholtz Zentrum München, Munich, Germany

⁹ These authors contributed equally to this work.

Introduction

Transmissible spongiform encephalopathies (TSEs) are fatal neurodegenerative disorders that affect humans and various mammals including cattle, sheep, deer, and elk. TSEs are characterized by the conversion of the cellular prion protein (PrP^C) into a misfolded isoform termed PrP^{Sc} [1]. PrP^{Sc} aggregation is associated with gliosis, spongiosis, and neurodegeneration [2] which invariably leads to death. Prion diseases have been long known to be transmissible [3], and prion transmission can occur after oral, corneal, intraperitoneal (i.p.), intravenous (i.v.), intranasal (i.n.), intramuscular (i.m.), intralingual, transdermal and intracerebral (i.c.) application, the most efficient being i.c. inoculation [4,5,6,7,8,9,10,11,12]. Several biological fluids and excreta (e.g. saliva, milk, urine, blood, placenta, feces) contain significant levels of prion infectivity [13,14,15,16,17], and horizontal transmission is believed to be critical for the natural spread of TSEs [18,19,20,21,22,23]. Free-ranging animals may absorb infectious prion particles through feeding or drinking [24,25], and tongue wounds may represent entry sites for prions [26].

PrP^{Sc} has also been found in the olfactory epithelium of sCJD patients [27,28]. Prion colonization of the nasal epithelium occurs in various species and with various prion strains [11,12,29,30,31,32,33,34,35,36,37]. In the HY-TME prion model, intranasal application is 10–100 times more efficient than oral uptake [29] and, as in many other experimental paradigms [38,39,40,41,42,43,44], the lymphoreticular system (LRS) is the earliest site of PrP^{Sc} deposition. A publication demonstrated transmission of chronic wasting disease (CWD) in cervidized mice via aerosols and upon intranasal inoculation [45], yet two studies reported diametrically differing results on the role of the olfactory epithelium or the LRS in prion pathogenesis upon intranasal prion inoculation [11,12], perhaps because of the different prion strains and animal models used. These controversies indicate that the mechanisms of intranasal and aerosolic prion infection are not fully understood. Furthermore, intranasal administration is physically very different from aerial prion transmission, as the airway penetration of prion-laden droplets may be radically different in these two modes of administration.

Here we tested the cellular and molecular characteristics of prion propagation after aerosol exposure and after intranasal

Author Summary

Prions, which are the cause of fatal neurodegenerative disorders termed transmissible spongiform encephalopathies (TSEs), can be experimentally or naturally transmitted via prion-contaminated food, blood, milk, saliva, feces and urine. Here we demonstrate that prions can be transmitted through aerosols in mice. This also occurs in the absence of immune cells as demonstrated by experiments with mice lacking B-, T-, follicular dendritic cells (FDCs), lymphotoxin signaling or with complement-deficient mice. Therefore, a functionally intact immune system is not strictly needed for aerogenic prion infection. These results suggest that current biosafety guidelines applied in diagnostic and scientific laboratories ought to include prion aerosols as a potential vector for prion infection.

instillation. We found both inoculation routes to be largely independent of the immune system, even though we used a strongly lymphotropic prion strain. Aerosols proved to be efficient vectors of prion transmission in mice, with transmissibility being mostly determined by the exposure period, the expression level of PrP^C, and the prion titer.

Results

Prion transmission via aerosols

Prion aerosols were produced by a nebulizing device with brain homogenates at concentrations of 0.1–20% (henceforth always indicating weight/volume percentages) derived from terminally scrapie-sick or healthy mice, and inhaled into an inhalation chamber. As per the manufacturer's specifications, aerosolized particles had a maximal diameter of <10 μm , and approximately 60% were <2.5 μm [46].

Groups of mice overexpressing PrP^C (*tga20*; $n=4-7$) were exposed to prion aerosols derived from infectious or healthy brain homogenates (henceforth IBH and HBH) at various concentrations (0.1, 2.5, 5, 10 and 20%) for 10 min (Fig. 1A, Table 1). All *tga20* mice exposed to aerosols derived from IBH (concentration: $\geq 2.5\%$) succumbed to scrapie with an attack rate of 100%. The incubation time negatively correlated with the IBH concentration (2.5%: $n=4$, 165 ± 54 dpi; 5%: $n=4$, 131 ± 7 dpi; 10%: $n=5$, 161 ± 27 dpi; 20%: $n=6$, 133 ± 8 dpi; $p=0.062$, standard linear regression on standard ANOVA; Fig. 1A and F, Table 1, Table S1A).

tga20 mice exposed to aerosolized 0.1% IBH did not develop clinical scrapie within the observational period ($n=4$; experiment terminated after 300 dpi), yet displayed brain PrP^{Sc} indicative of subclinical prion infection (Fig. 1A and 2A). In contrast, control *tga20* mice ($n=4$) exposed to aerosolized HBH did not develop any recognizable disease even when kept for ≥ 300 dpi, and their brains did not exhibit any PrP^{Sc} in histoblots and Western blots (data not shown).

In the above experiments, and in all experiments described in the remainder of this study, all PrP-expressing (*tga20* and WT) mice diagnosed as terminally scrapie-sick were tested by Western blot analysis and by histology: all were invariably found to contain PrP^{Sc} in their brains (Fig. 2) and to display all typical histopathological features of scrapie including spongiosis, PrP deposition and astrogliosis (Fig. 1H).

Correlation of exposure time to prion aerosols and incubation period

We then sought to determine the minimal exposure time that would allow prion transmission via aerosols (Fig. 1B, Table 1).

tga20 mice were exposed to aerosolized IBH (20%) for various durations (1, 5 or 10 min) in two independent experiments. Surprisingly, an exposure time of only 1 min was found to be sufficient to induce a 100% scrapie attack rate. Longer exposures to prion-containing aerosols strongly correlated with shortened incubation periods (Fig. 1B and G, Table 1, Table S1A and B).

In order to test the universality of the above results, we examined whether aerosols can transmit prions to various mouse strains (CD1, C57BL/6; 129SvxC57BL/6) expressing wild-type (wt) levels of PrP^C. CD1 mice were exposed to aerosolized 20% IBH in two independent experiments (Fig. 1C, Table 1). After 5 or 10-min exposures, all CD1 mice succumbed to scrapie whereas shorter exposure (1 min) led to attack rates of 0–50% [1 min exposure (first experiment): scrapie in 0/3 mice; 1 min exposure (second experiment): 2/4 mice died of scrapie at 202 ± 0 dpi; 5 min (first experiment): $n=4$, attack rate 100%, 202 ± 12 dpi; 5 min (second experiment): $n=3$, attack rate 100%, 202 ± 0 dpi; 10 min (first experiment): $n=4$, attack rate 100%, 202 ± 0 dpi; 10 min (second experiment): $n=4$, attack rate 100%, 206 ± 16 dpi]. In CD1 mice exposed to prion-containing aerosols for longer intervals, we detected a trend towards shortened incubation times which did not attain statistical significance (Table S1A and S1B).

We also investigated whether C57BL/6 or 129SvxC57BL/6 mice would succumb to scrapie upon exposure to prion aerosols (Fig. 1D and E, Table 1). A 10 min exposure time with a 20% IBH led to an attack rate of 100% (C57BL/6: 10 min: $n=4$; 185 ± 11 dpi; 129SvxC57BL/6: $n=5$; 10 min: 182 ± 15 dpi). Control *Pmp^{o/o}* mice (129SvxC57BL/6 background; $n=3$) were resistant to aerosolized prions (20%, 10 min) as expected (Fig. 1E and H, Table 1).

Incubation time and attack rate depends on PrP^C expression levels

When *tga20* mice were challenged for 10 min, variations in the concentration of aerosolized IBH had a barely significant influence on survival times ($p=0.062$; Fig. 1F), whereas variations in the duration of exposure of *tga20* mice affected their life expectancy significantly ($p<0.001$; Fig. 1G). Furthermore *tga20* mice, which express 6–9 fold more PrP^C in the central nervous system (CNS) than wt mice [46,47,48], succumbed significantly earlier to scrapie upon prion aerosol exposure for 10 min (20%) (*tga20* mice: 134 ± 4 dpi; CD1 mice: 202 ± 12 dpi, $p<0.0001$; C57BL/6 mice: 185 ± 11 dpi, $p=0.003$; 129SvxC57BL/6 mice: 182 ± 15 dpi, $p=0.003$; Fig. 1B–E, Fig. S1, Table S1A and S1C). Incubation time was prolonged and transmission was less efficient in CD1 mice than in *tga20* mice after a 1 min exposure to prion aerosols (20%). The variability of incubation times between CD1 mice was low (1st vs. 2nd experiment with 5-min exposure: $p=0.62$, 1st vs. 2nd experiment with 10-min exposure: $p=0.27$; Fig. 1C, Table 1). This suggests that 1 min exposure of CD1 mice to prion aerosols (20%) suffices for uptake of $\leq 1\text{LD}_{50}$ infectious units. This finding underscores the importance of PrP^C expression levels not only for the incubation time but also for susceptibility to infection and neuroinvasion upon exposure to aerosols. Histoblot analyses confirmed deposition of PrP^{Sc} in brains of *tga20* mice exposed to prion aerosols derived from 10% or 20% IBH, whereas no PrP^{Sc} was found in brains of *Pmp^{o/o}* mice exposed to prion aerosols (Fig. 2D).

We then performed a semiquantitative analysis of the histopathological lesions in the CNS. The following brain regions were evaluated according to a standardized severity score (astrogliosis, spongiform change and PrP^{Sc} deposition; [49]): hippocampus, cerebellum, olfactory bulb, frontal white matter, and temporal white matter. Scores were compared to those of

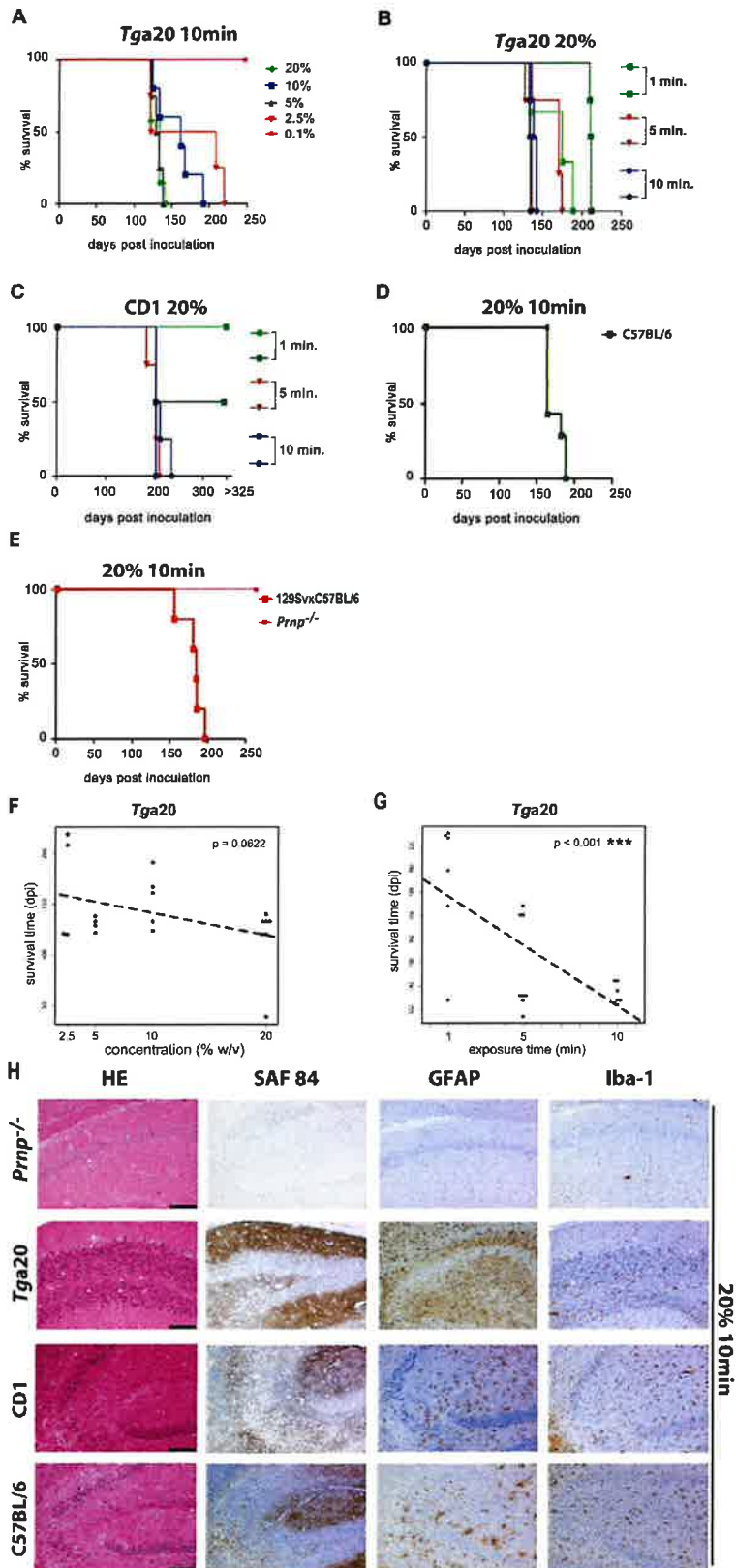


Figure 1. Prion transmission through aerosols. (A) *tga20* mice were exposed to aerosols generated from 0.1%, 2.5%, 5%, 10% or 20% prion-infected mouse brain homogenates (IBH) for 10 min. (B) Groups of *tga20* and (C) CD1 mice were exposed for 1, 5 or 10 min to aerosols generated from a 20% IBH. Experiments were performed twice (different colors). (D) C57BL/6, (E) 129SvxC57BL/6, and *Prnp^{0/0}* mice were exposed for 10 min to aerosols generated from 20% IBH. Kaplan-Meier curves describe the percentage of survival after particular time points post exposure to prion aerosols (y-axis represents percentage of living mice; x-axis demonstrates survival time in days post inoculation). Different colors and symbols describe the various experimental groups. (F) Jittered scatter plot of survival time against concentration of prion aerosols generated out of IBH with added linear regression fit ($p = 0.0622$). (G) Jittered scatter plot of survival time against exposure time for *tga20* mice with added linear regression fit. The negative correlation between survival time and exposure time is significant ($p < 0.001^{***}$). (H) Consecutive paraffin sections of the right hippocampus of *Prnp^{0/0}*, *tga20*, CD1 and C57BL/6 mice stained with HE (for spongiosis, gliosis, neuronal cell loss), SAF84 (PrP^{Sc} deposits), GFAP (astroglia) and Iba-1 (microglia). All animals had been exposed to aerosols generated from 20% IBH for 10 min. Scale bars: 100µm. doi:10.1371/journal.ppat.1001257.g001

mice inoculated i.c. with RML (Fig. 2E and F). Lesion profiles of terminally scrapie-sick mice (*tga20*, CD1, C57BL/6 and 129SvxC57BL/6) infected i.c. or through aerosols were similar irrespectively of genetic background or PrP^C expression levels (Fig. 2E and F), with CD1 and 129SvxC57BL/6 hippocampi and cerebella displaying only mild histological and immunohistochemical features of scrapie regardless of the route of inoculation.

We attempted to trace PrP^{Sc} in the nasopharynx, the nasal cavity or various brain regions early after prion aerosol infection (1–6 hrs post exposure) and at various time points after intranasal inoculations (6, 12, 24, 72, 144 hrs, 140 dpi, and terminally) with various methods including Western blot, histoblot and protein misfolding analyses. However, none of these analyses detected PrP^{Sc} shortly after exposure to prion aerosols (6–72 hrs post prion aerosol exposure) whereas at 140 dpi or terminal stage PrP^{Sc} was detected by all of these methods (Fig. S2; data not shown).

PrP^C expression on neurons allows prion neuroinvasion upon infection with prion aerosols

We then investigated whether PrP^C expression in neurons would suffice to induce scrapie after exposure to prions through aerosols. *NSE-PrP* transgenic mice selectively express PrP^C in neurons and if bred on a *Prnp^{0/0}* background (*Prnp^{0/0}/NSE-PrP*) display CNS-restricted PrP expression levels similar to wt mice [50].

Prnp^{0/0}/NSE-PrP (henceforth referred to as *NSE-PrP*) mice were exposed to prion aerosols (20% homogenate; 10 min). All *NSE-PrP* mice succumbed to terminal scrapie (216 ± 8 dpi; $n = 4$; Fig. 1E, 2G, Table 1), although incubation times were significantly longer than those of wt 129SvxC57BL/6 mice (180 ± 15 dpi; $n = 5$; $p = 0.004$). Histology and immunohistochemistry confirmed scrapie in *NSE-PrP* brains (Fig. 2H and I). Histopathological lesion severity score analysis (see above) revealed a lesion profile roughly

Table 1. Survival times of different mouse strains exposed to prion aerosols for various periods.

Genotype	inoculum concentr.	exposure (min)	n	attack rate	Incubation time (dpi)					
<i>tga20</i>	0.1%	10	4	0/4	>300	>300	>300	>300		
<i>tga20</i>	2.5%	10	4	4/4	120	121	208	219		
<i>tga20</i>	5%	10	4	4/4	122	129	133	138		
<i>tga20</i>	10%	10	5	5/5	124	133	161	167	191	
<i>tga20</i>	20%	10	6	6/6	120	120	133	133	133	140
CD1	20%	1	3	0/3	>300	>300	>300			
CD1*	20%	1	4	2/4	202	202	>300	>300		
<i>tga20</i>	20%	1	3	3/3	134	174	189			
<i>tga20*</i>	20%	1	3	3/3	203	204	205			
CD1	20%	5	4	4/4	182	202	202	209		
CD1*	20%	5	3	3/3	202	202	202			
<i>tga20</i>	20%	5	4	4/4	136	170	170	174		
<i>tga20*</i>	20%	5	4	4/4	127	134	136	136		
CD1	20%	10	4	4/4	202	202	202	202		
CD1*	20%	10	4	4/4	202	202	211	235		
<i>tga20</i>	20%	10	4	4/4	134	138	142	142		
<i>tga20*</i>	20%	10	4	4/4	132	133	134	134		
C57BL/6	20%	10	4	4/4	164	182	188	188		
129SvxC57BL/6	20%	10	5	5/5	155	180	182	184	197	
<i>Prnp^{0/0}</i>	20%	10	3	0/3	>300	>300	>300			
newborn <i>tga20</i>	20%	10	3	3/3	157	189	189			
newborn CD1	20%	10	3	3/3	211	211	211			

Upper panel: survival times of *tga20* mice after 10-min exposure to aerosols generated from various concentrations of IBH. Lower panel: survival times of various mouse strains after exposure for 1, 5, or 10 min to infectious aerosols. Selected inoculations were repeated sequentially (asterisks) in order to estimate the reproducibility of these results.

doi:10.1371/journal.ppat.1001257.t001

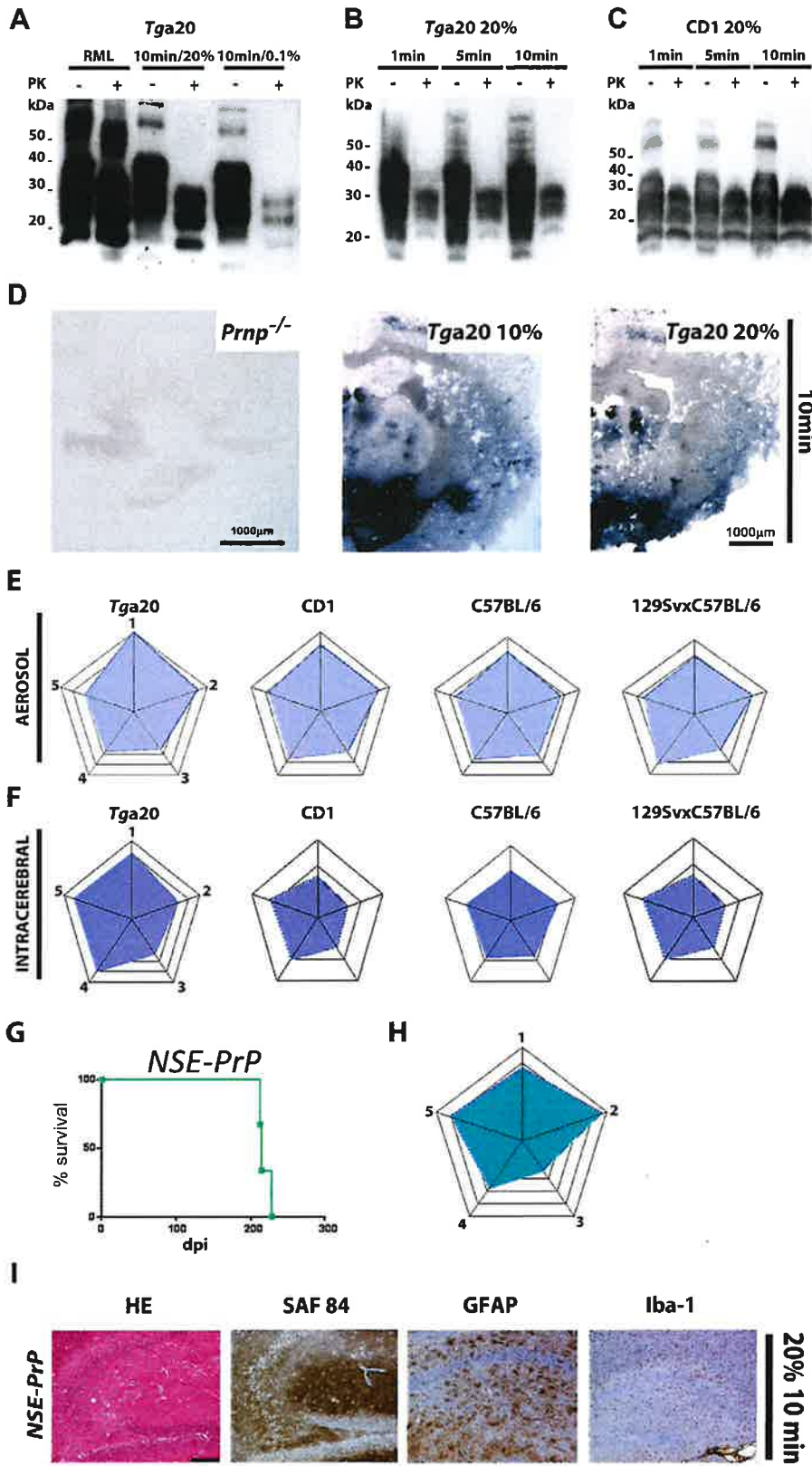


Figure 2. PrP^{Sc} deposition in brains of mice infected with prion aerosols and profiling of *NSE-PrP* mice. (A) Western blot analysis of brain homogenates (10%) from terminal or subclinical *tga20* mice exposed to aerosols from 20% or 0.1% IBH for 10 min. PK+ or -: with or without proteinase K digest; kDa: Kilo Dalton. (B–C): Western blot analyses of brain homogenates from *tga20* (B) or CD1 (C) mice exposed to prion aerosols from 20% IBH. (D) Histoblot analysis of brains from mice exposed to prion aerosols. Brains of *tga20* mice challenged with aerosolized 10% (middle panel) or 20% (right panel) IBH showed deposits of PrP^{Sc} in the cortex and mesencephalon. Because the brain of a *Prnp*^{0/0} mouse showed no signal (left panel), we deduce that the signal in the middle and right panels represents local prion replication. (E) Histopathological lesion severity score analysis of 5 brain regions depicted as radar plots [51] (astrogliosis, spongiform change and PrP^{Sc} deposition) derived from *tga20*, CD1, C57BL/6 and 129SvxC57BL/6 mice exposed to prion aerosols. Numbers correspond to the following brain regions: (1) hippocampus, (2) cerebellum, (3) olfactory bulb, (4) frontal white matter, (5) temporal white matter. (F) Histopathological lesion severity score of 5 brain regions shown as radar blot (astrogliosis, spongiform change and PrP^{Sc} deposition) of i.c. prion inoculated *tga20*, CD1, C57BL/6 and 129SvxC57BL/6 mice. (1) hippocampus, (2) cerebellum, (3) olfactory bulb, (4) frontal white matter, (5) temporal white matter. (G) Survival curve and (H) lesion severity scores of *NSE-PrP* mice exposed to a 20% aerosolized IBH for 10 min. (I) Histological and immunohistochemical characterization of scrapie-affected hippocampi of *NSE-PrP* mice after exposure to aerosolized 20% IBH. Stain legend as in Fig. 1H. Scale bar: 100µm. doi:10.1371/journal.ppat.1001257.g002

similar to that of control 129SvxC57BL/6 mice (Fig. 2E, H). More severe lesions were observed in *NSE-PrP* cerebella whereas olfactory bulbs were less affected.

Real time PCR analysis revealed 2–4 transgene copies per *Prnp* allele in *Prnp*^{0/0}/*NSE-PrP* mice.

A detailed quantitative analysis of PrP^C expression levels at various sites of the CNS was performed by comparing the signals obtained by blotting various amounts of protein from *NSE-PrP*, wt and *tga20* tissues (Fig. S3). A value of 100 was arbitrarily assigned to expression of PrP^C in wt tissues; olfactory epithelia of *tga20* and *NSE-PrP* mice expressed ≥ 350 and ~ 30 , respectively (Fig. S3A). In olfactory bulbs, *tga20* and *NSE-PrP* mice expressed ≥ 150 and 30, respectively (Fig. S3B). In brain hemispheres *tga20* and *NSE-PrP* mice expressed > 250 and > 150 , respectively (Fig. S3C). Therefore, *NSE-PrP* mice expressed somewhat more PrP^C than wt mice in brain hemispheres, but somewhat less in olfactory bulbs and olfactory epithelia.

Aerosolic prion infection is independent of the immune system

In many paradigms of extracerebral prion infection, efficient neuroinvasion relies on the anatomical and physiological integrity of several immune system components [40,42,43,44]. To determine whether this is true for aerosolic prion challenges, we exposed immunodeficient mouse strains to prion aerosols. This series of experiments included *JH*^{-/-} mice, which selectively lack B-cells, and γ_c *Rag2*^{-/-} mice which are devoid of mature B-, T- and NK-cells (Fig. 3A). Upon exposure to prion aerosols (20% IBH; exposure time 10 min) both *JH*^{-/-} and γ_c *Rag2*^{-/-} mice succumbed to scrapie with a 100% attack rate (*JH*^{-/-}: n=6, 181±21 dpi; γ_c *Rag2*^{-/-}: n=11, 185±41 dpi, $p=0.65$). The incubation times were not significantly different to those of C57BL/6 wt mice exposed to prion aerosols (*JH*^{-/-} mice: $p=0.9$; γ_c *Rag2*^{-/-} mice: $p=0.7$).

Histological and immunohistochemical analyses confirmed scrapie in all clinically diagnosed mice. Lesion severity score analyses (Fig. 3A and 3E) showed that *JH*^{-/-} and γ_c *Rag2*^{-/-} mice had lower profile scores in cerebella and higher scores in hippocampi and frontal white matter than C57BL/6 mice. Slightly higher scores in temporal white matter areas and the thalamus could be detected in *JH*^{-/-} and γ_c *Rag2*^{-/-} mice, whereas γ_c *Rag2*^{-/-} mice showed lower scores in olfactory bulbs. Consistently with several previous reports, γ_c *Rag2*^{-/-} mice (n=4) did not succumb to scrapie after i.p. prion inoculation (100µl RML6 0.1% 6 log LD50) even when exposed to a prion titer that was twice higher than that used for intranasal inoculations (data not shown).

Depending on the exposure time and the IBH concentration, *tga20* mice developed splenic PrP^{Sc} deposits. In contrast, none of the scrapie-sick *JH*^{-/-}, *LTβR*^{-/-} and γ_c *Rag2*^{-/-} mice displayed

any splenic PrP^{Sc} on Western blots and/or histoblots (Fig. S4A–D) despite copious brain PrP^{Sc}.

Aerosol infection is independent of follicular dendritic cells

Follicular dendritic cells (FDCs) are essential for prion replication within secondary lymphoid organs and for neuroinvasion after i.p. or oral prion challenge [42,44,51]. Lymphotoxin beta receptor-Ig fusion protein (LTβR-Ig) treatment in C57BL/6 mice causes dedifferentiation of mature FDCs, resulting in reduced peripheral prion replication and neuroinvasion upon extraneural (e.g. intraperitoneal or oral) prion inoculation [52,53]. We therefore investigated whether FDCs are required for prion replication after challenge with prion aerosols. C57BL/6 mice were treated with LTβR-Ig or nonspecific pooled murine IgG (muIgG) before and after prion challenge (-7, 0, and +7 days) (Fig. 3B). The effects of the LTβR-Ig treatment were monitored by Mfg-E8⁺/FDC-M1⁺ staining for networks of mature FDCs in lymphoid tissue. This analysis revealed a complete loss of Mfg-E8⁺/FDC-M1⁺ networks at the day of prion exposure and at 14 dpi (data not shown).

LTβR-Ig treatment and dedifferentiation of FDCs did not alter incubation times upon aerosol prion infection (LTβR-Ig: n=3, attack rate 100%, 184±0 dpi; muIgG: n=3, attack rate 100%, 184±0 dpi) (Fig. 3B, Table 2). The diagnosis of terminal scrapie was confirmed by histological and immunohistochemical analyses in all clinically affected mice (Fig. 3B; data not shown). Histopathological lesion severity scoring revealed that LTβR-Ig treated C57BL/6 mice displayed a higher score in all regions investigated than untreated C57BL/6 mice upon challenge with prion aerosols (20% IBH; 10 min) (Fig. 2E and 3B). We found slightly less severe scores in the olfactory bulbs of C57BL/6 mice treated with muIgG than in untreated C57BL/6 mice upon challenge with prion aerosols (Fig. 2E and 3B), and a slightly higher score in the temporal white matter (exposure to 20% aerosol for 10 min; Fig. 2E and 3B).

Prion aerosol infection of mice lacking LTβR or CD40L

LTβR signaling is essential for proper development of secondary lymphoid organs and for maintenance of lymphoid microarchitecture, and was recently shown to play an important role in prion replication within ectopic lymphoid follicles and granulomas [40,41,44]. To investigate the role of this pathway in aerogenic prion infections, *LTβR*^{-/-} mice were exposed to prion aerosols (20% IBH; 10 min exposure time). All *LTβR*^{-/-} mice succumbed to scrapie (*LTβR*^{-/-}: n=4, 272±0 dpi) and displayed PrP deposits in their brains (Fig. 3C). Histological severity scoring of aerosol-exposed mice revealed higher scores in *LTβR*^{-/-} hippocampi and lower scores in cerebellum, olfactory bulb, frontal and temporal white matter than in C57BL/6 controls (exposure: 20%; 10 min; Fig. 2E and 3C).

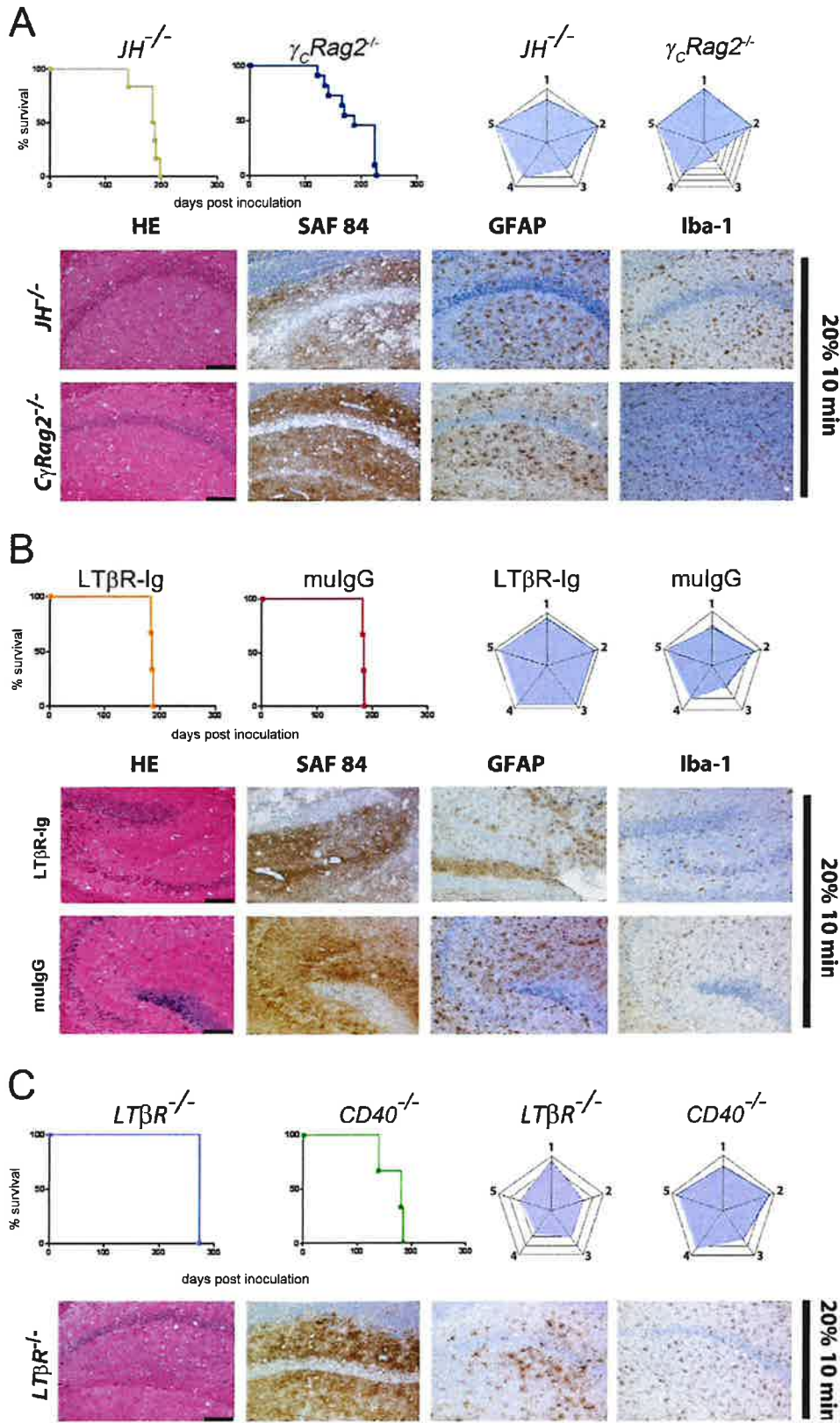


Figure 3. Prion transmission through aerosols in immunocompromised mice. Survival curves, lesion severity score analysis (radar plots), and representative histopathological micrographs of mice with genetically or pharmacologically impaired components of the immune system (*JH*^{-/-}, *γC*Rag2^{-/-} **A**), 129Sv mice treated with LTβR-Ig or with mulgG (**B**), and *LTβR*^{-/-}, and *CD40*^{-/-} mice (**C**). All mice were exposed for 10 min to aerosolized 20% IBH. Stain code: HE (spongiosis, gliosis, neuronal cell loss), SAF84 (PrP^{Sc} deposits), GFAP (astrogliosis) and Iba-1 (microglial activation) as in Fig. 1H. Scale bars: 100μm.
doi:10.1371/journal.ppat.1001257.g003

We then investigated the role of CD40 receptor in prion aerosol infection. *CD40*^{-/-} mice fail to develop germinal centers and memory B-cell responses, yet *CD40L*^{-/-} mice show unaltered incubation times upon i.p. prion challenge [54]. Similarly to the other immunocompromised mouse models investigated, *CD40*^{-/-} mice developed terminal scrapie upon infection with prion aerosols with an attack rate of 100% (n = 3, 276 ± 50 dpi). Lesion severity analyses of *CD40*^{-/-} mice revealed a slightly higher score in the cerebellum and the temporal white matter than in C57BL/6 mice (Fig. 2E and 3C). Therefore, LTβR and CD40 signaling are dispensable for aerosolic prion infection.

Components of the complement system are dispensable for aerosolic prion infection

Certain components of the complement system (e.g. C3; *C1qa*) play an important role in early prion uptake, peripheral prion replication and neuroinvasion after peripheral prion challenge [43,55,56]. We have tested whether this is true also for exposure to prion aerosols. Mice lacking both complement components C3 and C4 (*C3C4*^{-/-}) were exposed for 10 min to 20% aerosolized IBH. All *C3C4*^{-/-} mice succumbed to scrapie (n = 3, 382 ± 33 dpi; Fig. 4A). Histopathological evaluation of all scrapie affected mice revealed astrogliosis, spongiform changes and PrP-deposition in the CNS (Fig. 4A).

Table 2. Survival of mouse strains exposed to prion aerosols (upper panel) or intranasal administered prions (lower panel).

Genotype	n	Attack rate	Survival (dpi)										
Aerosol (20% IBH)													
NSE-Prp	4	4/4	211	211	213	227							
<i>JH</i> ^{-/-}	6	6/6	140	184	184	188	190	198					
<i>γC</i> Rag2 ^{-/-}	11	11/11	121	134	141	165	169	187	224	224	224	224	227
C57BL/6 treated with LTβR-Ig	3	3/3	184	184	184								
C57BL/6 treated with mulgG	3	3/3	184	184	184								
<i>LTβR</i> ^{-/-}	4	4/4	272	272	272	272							
<i>CD40</i> ^{-/-}	3	3/3	220	292	315								
<i>C3</i> ^{-/-} <i>C4</i> ^{-/-}	3	3/3	363	363	420								
Intranasal inoculation													
<i>Prnp</i> ^{0/0}	8	0/8	>300	>300	>300	>300	>300	>300	>300	>300	>300	>300	>300
C57BL/6	8	8/8	219	219	253	263	292	292	292	292	296		
129SvxC57BL/6	5	5/5	187	213	213	235	235						
Balb/c	6	6/6	112	225	225	225	225	242					
<i>tga20</i>	10	10/10	118	125	126	133	152	165	186	187	202	203	
NSE-Prp	6	6/6	201	230	255	267	383	411					
<i>Rag1</i> ^{-/-}	9	9/9	198	198	198	200	203	203	204	210	214		
<i>γC</i> Rag2 ^{-/-}	16	16/16	224	224	224	229	241	242	242	242	244		
			244	256	258	264	265	265	319				
<i>C1qa</i> ^{-/-}	4	4/4	256	284	291	319							
<i>CD21</i> ^{-/-}	10	10/10	212	212	214	216	226	235	236	263	269	270	
<i>CXCR5</i> ^{-/-}	5	5/5	190	245	363	363	403						
C57BL/6 treated with LTβR-Ig	8	8/8	219	222	407	413	475	638	717	717			
C57BL/6 treated with mulgG	9	9/9	176	242	242	242	255	255	263	271	272		
<i>LTβR</i> ^{-/-}	6	6/6	223	252	263	314	346	348					
<i>TNFR1</i> ^{-/-}	3	3/3	213	213	214								
<i>LTα</i> ^{-/-}	6	6/6	233	234	238	255	262	283					
C57BL/6 HBH	4	0/4	>300	>300	>300	>300							
Balb/c HBH	4	0/4	>300	>300	>300	>300							
<i>Rag1</i> ^{-/-} HBH	4	0/4	>300	>300	>300	>300							
<i>γC</i> Rag2 ^{-/-} HBH	4	0/4	>300	>300	>300	>300							

doi:10.1371/journal.ppat.1001257.t002

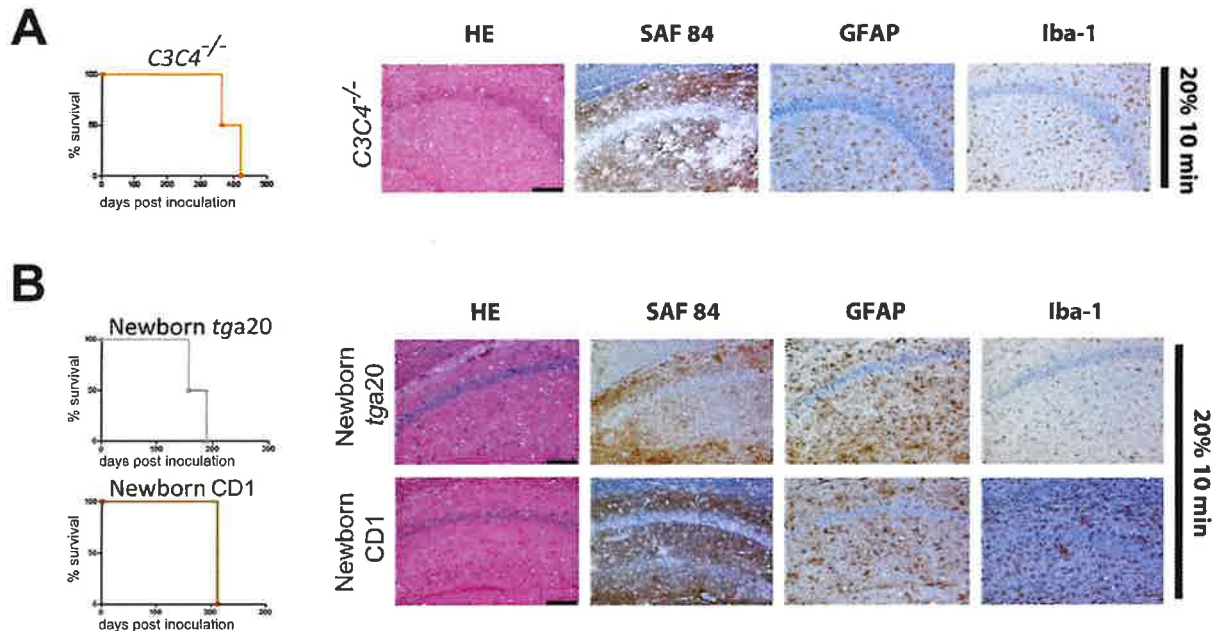


Figure 4. Prion transmission through aerosols in complement-deficient and newborn mice. (A) *C3C4*^{-/-} mice and (B) newborn *tga20* and CD1 mice were exposed for 10 min to a 20% aerosolized IBH. Survival curves (right panels) as well as histological and immunohistochemical characterization of hippocampi indicate that all prion-exposed mice developed scrapie efficiently. Scale bars: 100µm. doi:10.1371/journal.ppat.1001257.g004

No protection of newborn mice against prion aerosols

The data reported above argued in favor of direct neuroinvasion via PrP^C-expressing neurons upon aerosol administration. However, a possible alternative mechanism of transmission may be via the ocular route, namely via cornea, retina, and optic nerve [57,58]. In order to test this possibility, newborn (<24 hours-old) *tga20* and CD1 mice, whose eyelids were still closed, were exposed for 10 min to prion aerosols generated from a 20% IBH. All mice succumbed to scrapie and showed PrP deposits in brains (*tga20* mice: n = 3, 173 ± 23 dpi; CD1 mice: n = 3, 211 ± 0 dpi) (Fig. 4B). Newborn *tga20* mice succumbed to scrapie slightly later ($p = 0.0043$) than adult *tga20* mice, whereas no differences were observed between newborn and adult CD1 mice exposed for 10 min to prion aerosols generated from a 20% IBH ($p = 0.392$).

The brains of all animals contained PK-resistant material, as evaluated by Western blot analysis (data not shown). In addition, untreated littermates or other sentinels which were reared or housed together with aerosol-treated mice immediately following exposure to aerosols showed neither signs of scrapie nor PrP^{Sc} in brains, even after 482 dpi. This suggests that prion transmission was the consequence of direct exposure of the CNS to prion aerosols rather than the result of transmission via other routes like ingestion from fur by grooming or exposure to prion-contaminated feces or urine.

Lack of PrP^{Sc} in secondary lymphoid organs of immunocompromised, scrapie-sick mice after infection with prion aerosols

We further investigated additional mice for the occurrence of PrP^{Sc} in secondary lymphoid organs upon exposure to prion aerosols. PK-resistant material was searched for in spleens, bronchial lymph nodes (bln) and mesenteric lymph nodes (mln) at terminal stage of disease. C57BL/6, 129SvxC57BL/6, muIgG

treated C57BL/6 mice, newborn *tga20* mice as well as newborn CD1 mice contained PrP^{Sc} in the LRS, whereas LTβR^{-/-} mice and C57BL/6 mice treated with LTβR-Ig lacked PrP^{Sc} deposits in spleens (Fig. S4A–F; Table 3).

The efficiency of intranasal prion inoculation depends on the level of PrP^C expression

To dissect aerosol-mediated from non-aerosolic contributions to prion exposure, we directly applied a prion suspension (RML 6.0, 0.1%, 40µl, corresponding to 4 × 10⁵ LD₅₀ scrapie prions) to the nasal mucosa of various mouse lines (Fig. S5). Since mice breathe exclusively through their nostrils [59,60] we reasoned that this procedure would simulate aerosolic transmission with sufficient faithfulness although the mechanisms of prion uptake could still differ between aerosolic and intranasal administration [11].

tga20 (n = 10), 129SvxC57BL/6 (n = 5), C57BL/6 (n = 8) and *Prnp*^{0/0} mice (n = 8) were challenged intranasally with prions (Fig. S5). To test the possibility that the inoculation procedure itself might impact the life expectancy of mice, C57BL/6 mice (n = 4) were inoculated intranasally with healthy brain homogenate (HBH) for control (Fig. S5E). None of the animals that had been inoculated with HBH displayed a shortened life span, nor did they develop any clinical signs of disease - even when kept for ≥500 dpi. In contrast, after intranasal prion inoculation all C57BL/6, 129SvxC57BL/6 and *tga20* mice succumbed to scrapie with an attack rate of 100% (Fig. S5A–C), whereas *Prnp*^{0/0} mice were resistant to intranasal prions (Fig. S5D). After intranasal inoculation, *tga20* mice (n = 10, 160 ± 28 dpi) displayed a shorter incubation time (Fig. S5C) than 129SvxC57BL/6 (n = 5, 217 ± 20 dpi) or C57BL/6 mice (n = 8, 266 ± 33 dpi; Fig. S5A and S5B). Further, histological and immunohistochemical analyses for spongiosis, astrogliosis and PrP deposition pattern confirmed terminal scrapie (Fig. S5J). A histopathological lesion severity score

Table 3. PrP^{Sc} deposition in spleens of mice challenged with a range of aerosolized prion concentrations and exposure times.

Genotype	Splenic PrP ^{Sc} in individual mice										
	#1	#2	#3	#4	#5	#6	#7	#8	#9	#10	#11
<i>Prnp</i> ^{0/0}	-	-	-								
Newborn CD1 (20%; 10 min exp.)	+	+	+								
CD1 (20%; 1 min exp.)	+	+	+	+	-	Nd	Nd				
CD1 (20%; 5 min exp.)	+	+	-	-	+	Nd	Nd				
CD1 (20%; 10 min exp.)	+	+	+	+	+	Nd	Nd	Nd			
C57BL/6 (20%; 10 min exp.)	+	+	+	+							
129SvxC57BL/6 (20%; 10 min exp.)	+	+	+	+	+						
Newborn <i>tga20</i> (20%; 10 min exp.)	+	+	+								
<i>tga20</i> (0.1%; 10 min exp.)	-	-	-	-							
<i>tga20</i> (2.5%; 10 min exp.)	+	+	+	+							
<i>tga20</i> (5%; 10 min exp.)	+	+	+	+							
<i>tga20</i> (10%; 10 min exp.)	+	+	+	+	Nd						
<i>tga20</i> (20%; 1 min exp.)	+	+	+	+	-	-					
<i>tga20</i> (20%; 5 min exp.)	+	+	+	+	+	+	Nd	Nd			
<i>tga20</i> (20%; 10 min exp.)	+	+	+	+	+	+	+	+			
<i>tga20</i> (20%; 10 min exp.)	+	+	+	+	+	+	+	+			
JH ^{-/-}	-	-	-	-							
γ C $Rag2$ ^{-/-}	-	-	-	-	-	-	-	-	-	-	-
C57BL/6 treated with LTBR-Ig	-	-	-								
C57BL/6 treated with mu-IgG	+	+	Nd								
LTBR ^{-/-}	-	-	-	-							

PrP^{Sc} was assessed on Western blots and histoblots of spleens of *Prnp*^{0/0}, newborn CD1, adult CD1, 129SvxC57BL/6, newborn *tga20*, adult *tga20*, JH^{-/-}, γ C $Rag2$ ^{-/-}, C57BL/6 mice treated with LTBR-Ig or muIgG and LTBR^{-/-} mice. +: PrP^{Sc} detectable in spleen; -: PrP^{Sc} undetectable; Nd: not determined; exp.: exposure time (minutes). doi:10.1371/journal.ppat.1001257.t003

analysis revealed similar lesion profiles as detected after exposure to prion aerosols (Fig. S5K). However, in the olfactory bulb of *tga20* and 129SvxC57BL/6 mice the score was lower upon intranasal administration than in the aerosol paradigm (Fig. 2E).

Finally, we tested whether prion transmission via the intranasal route would be enabled by selective PrP^{Sc} expression on neurons. For that, we inoculated *NSE-PrP* mice. All intranasally challenged *NSE-PrP* mice (n=6, 291±86 dpi) succumbed to scrapie. The incubation time until terminal disease did not differ significantly from that of 129SvxC57BL/6 control mice (n=5, 217±20 dpi; $p=0.0868$).

Intranasal prion transmission in the absence of a functional immune system

Next, we sought to determine which components (if any) of the immune system are required for neuroinvasion upon intranasal infection with prions. To address this question, *Rag1*^{-/-} and γ C $Rag2$ ^{-/-} mice were intranasally inoculated with prions (inoculum RML 6.0, 0.1%, 40 μ l, equivalent to 4×10⁵ LD₅₀ scrapie prions). Remarkably, all intranasally prion-inoculated *Rag1*^{-/-} (n=9, 203±6 dpi) (Fig. 5A and H) and γ C $Rag2$ ^{-/-} mice (n=16, 243±24 dpi) (Fig. 5D and G) succumbed to scrapie, providing evidence for a LRS-independent mechanism of prion neuroinvasion upon intranasal administration. Incubation times in *Rag1*^{-/-} were significantly different to those of intranasally challenged control mice (C57BL/6; attack rate 100%; n=8, 266±33 dpi; $p=0.0009$) whereas γ C $Rag2$ ^{-/-} mice were not different from those of intranasally challenged control mice

(Balb/c: attack rate 100%, n=6, 209±48 dpi, $p=0.099$) (Fig. 5B and Fig. 5D).

After intranasal prion administration, PrP^{Sc} was present in the CNS of *Rag1*^{-/-} or γ C $Rag2$ ^{-/-} mice. WB analysis corroborated terminal scrapie (Fig. 5G and H). Histopathological lesion severity scoring revealed a distinct lesion profile characterized by a high score in the temporal white matter and the thalamus in case of *Rag1*^{-/-} mice. In case of γ C $Rag2$ ^{-/-} mice the cerebellum, the olfactory bulb and the frontal white matter displayed lower scores (Fig. 5I and J). In contrast to the CNS spleens of the affected animals did not contain PK-resistant material in terminally sick *Rag1*^{-/-} and γ C $Rag2$ ^{-/-} mice (Fig. S6E).

For control, *Rag1*^{-/-} as well as γ C $Rag2$ ^{-/-} mice were intranasally inoculated with HBH to test the possibility that intranasal inoculation itself impacts their life expectancy. None of the mice inoculated with HBH died spontaneously or developed scrapie up to ≥ 300 dpi (n=4 each; Fig. S6A, C–D). Further, Balb/c mice and C57BL/6 mice (n=4 each) inoculated intranasally with HBH (Fig. S5E and S6D) did not develop any disease for ≥ 300 dpi.

As a positive control, *Rag1*^{-/-} mice were i.c. inoculated with 3×10⁵ LD₅₀ scrapie prions. This led to terminal scrapie disease after approximately 130 days and an attack rate of 100% (n=3, 131±8 dpi) (Fig. 5B and data not shown).

As additional negative controls, *Rag1*^{-/-} and γ C $Rag2$ ^{-/-} mice were i.p. inoculated with prions (100 μ l RML 0.1%, 1×10⁶ LD₅₀). Although more infectious prions (approximately 2 fold more) were applied when compared to the intranasal route, i.p. prion

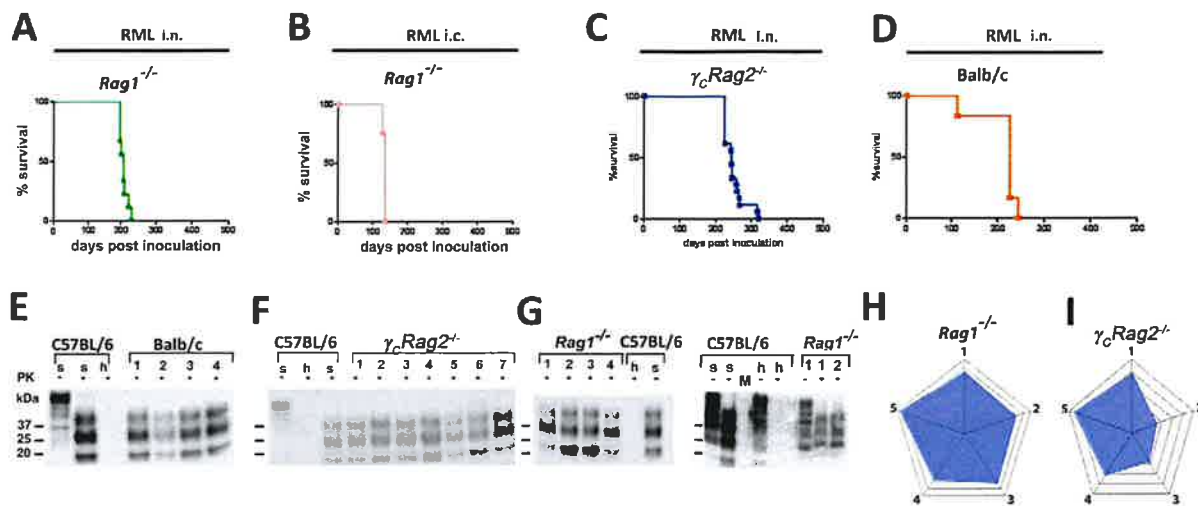


Figure 5. Prion transmission by intranasal instillation. (A) *Rag1*^{-/-} mice intranasally inoculated with RML6 0.1%, (B) C57BL/6 mice that have been intranasally inoculated with 3×10^5 LD₅₀ prions. (C) *Rag1*^{-/-} mice i.c. inoculated with 3×10^5 LD₅₀. (D) γ_C *Rag2*^{-/-} mice intranasally inoculated with 4×10^5 LD₅₀ or (E) Balb/c mice intranasally inoculated with 4×10^5 LD₅₀ scrapie prions are shown. Survival curves (A–D) and respective Western blots (F–G) are indicative of efficient prion neuroinvasion. Brain homogenates were analyzed with (+) and without (–) previous proteinase K (PK) treatment as indicated. Brain homogenates derived from a terminally scrapie-sick and a healthy C57BL/6 mouse served as positive and negative controls (s: sick; h: healthy), respectively. Molecular weights (kDa) are indicated on the left side of the blots. (H and I) Histopathological lesion severity score described as radar blot (astrogliosis, spongiform change and PrP^{Sc} deposition) in 5 brain regions of both mouse lines exposed to prion aerosols. Numbers correspond to the following brain regions: (1) hippocampus, (2) cerebellum, (3) olfactory bulb, (4) frontal white matter, (5) temporal white matter. doi:10.1371/journal.ppat.1001257.g005

inoculation did not suffice to induce scrapie in *Rag1*^{-/-} and γ_C *Rag2*^{-/-} mice (attack rate: 0%, n=4 for each group, experiment terminated after 400 dpi).

Relevance of the complement system for prion pathogenesis after intranasal challenge

The complement component *C1qa* is involved in facilitating the binding of PrP^{Sc} to complement receptors on FDCs [56]. Accordingly, *C1qa*^{-/-} mice are resistant to prion infection upon low-dose peripheral inoculation. *CD21*^{-/-} mice are devoid of the complement receptor 1, display a normal lymphoid microarchitecture and show a reduction in germinal center size. The incubation time in *CD21*^{-/-} mice is greatly increased upon peripheral prion inoculation via the i.p. route [56].

To determine whether the complement system is involved in prion infection through aerosols, *C1qa*^{-/-} and *CD21*^{-/-} mice were intranasally inoculated with prions. *C1qa*^{-/-} mice and *CD21*^{-/-} mice succumbed to scrapie with an attack rate of 100% (*C1qa*^{-/-} mice: n=4, 288±26 dpi; *CD21*^{-/-} mice: n=10, 235±24 dpi) (Figs. 6A–C), with *CD21*^{-/-} mice succumbing to scrapie slightly earlier when compared to *C1qa*^{-/-} mice. However, survival times did not differ significantly from C57BL/6 control mice (n=8, 266±33 dpi; *C1qa*^{-/-} mice: $p=0.24$; *CD21*^{-/-} mice: $p=0.05$) (Fig. S5A and S5B). Western blot analysis of one terminally scrapie-sick *C1qa*^{-/-} mouse revealed one PrP^{Sc} positive spleen (1/4) (Fig. S6F). Two terminally scrapie-sick *CD21*^{-/-} mice showed PK resistance in their spleens (2/10) (Fig. S6G). These results indicate that the complement components *C1qa* and *CD21* are not essential for prion propagation upon intranasal application.

CXCR5 deficiency does not shorten prion incubation time upon intranasal infection

CXCR5 controls the positioning of B-cells in lymphoid follicles, and the FDCs of CXCR5-deficient mice are in close proximity to

nerve terminals, leading to a reduced incubation time after i.p. prion inoculation [39,61]. Here we explored the impact of CXCR5 deficiency onto intranasal prion inoculation. *CXCR5*^{-/-} mice exhibited attack rates of 100%, and incubation times did not differ significantly from those of C57BL/6 mice (n=5, 313±91 dpi; $p=0.32$) (Fig. 6D). 3 out of 5 terminally scrapie-sick *CXCR5*^{-/-} mice revealed PK resistant material in their spleens (3/5), as detected by Western blot analysis (Fig. S6H).

Prion infection is independent of LTβR and TNFR1 signaling

Pharmacological inhibition of LTβR signaling strongly reduces peripheral prion replication and reduces or prevents prion neuroinvasion upon i.p. prion challenge [42,44,53]. To determine whether inhibition of LTβR signaling would affect prion transmission through the nasal cavity, we treated C57BL/6 mice with 100μg LTβR-Ig and for control with 100μg muIgG/mouse/week pre- and post-prion challenge (–7 days, 0 days, +7 days; 14 days). LTβR-Ig-treated mice were then inoculated intranasally with prions. 100% of the intranasally challenged mice died due to terminal scrapie (C57BL/6 mice treated with LTβR-Ig: n=8, 476±200 dpi; Fig. 7A). MuIgG treated mice served as controls and showed an insignificantly shortened incubation time (attack rate: 100%, n=9, 246±29 dpi) (Fig. 7B and C; C57BL/6 LTβR-Ig treated vs. muIgG treated mice: $p=0.014$; C57BL/6 untreated vs. LTβR-Ig treated C57BL/6 mice: $p=0.021$; C57BL/6 untreated vs. C57BL/6 muIgG treated mice: $p=0.22$).

We additionally challenged *LTβR*^{-/-}, *TNFR1*^{-/-} and *LTα*^{-/-} mice intranasally with RML prions (Fig. 7D–H). Under these conditions all *LTβR*^{-/-}, *TNFR1*^{-/-} and *LTα*^{-/-} mice developed terminal scrapie (*LTβR*^{-/-} mice: n=6, 291±52 dpi; *TNFR1*^{-/-} mice: n=3, 213±1 dpi; *LTα*^{-/-} mice: n=6, 251±20 dpi) (Fig. 7D–H). Terminal scrapie was confirmed by immunohistochemistry, histoblot and WB analysis (Fig. 7F and H, data not